COMMUNICATIONS IN NUMERICAL METHODS IN ENGINEERING, Vol. 10, 437–451 (1994)

NUMERICAL PROCEDURE FOR CALCULATION OF TEMPERATURE EVOLUTION IN COMPOSITE ELEMENTS WITH INTERNAL CAVITIES

P. LUYCKX, P. STIENON, J-M. FRANSSEN, J-C. DOTREPPE AND M. HOGGE
Université de Liège, Institut du Génie Civil, 6, quai Banning, 4000-Liège, Belgium

SUMMARY

In the paper a computation code based on the finite-element method for temperature evolutions in composite elements with internal cavities is presented. It is suitable for the analysis of various thermal problems encountered in mechanical and civil engineering such as fire risk assessment. It is based on a plane isoparametric triangular element with six nodes allowing the modelling of curved boundaries. In order to analyse composite steel–concrete elements and to take into account the non-linearities coming from the temperature-dependent material properties and from the boundary conditions, an implicit integration scheme is used. Another advantage of the program is the possibility of describing internal cavities with convection and radiation exchanges. In order to show the capacity of the program two examples are presented. Comparisons have been made with experimental and other numerical results, exhibiting very good agreement.

1. INTRODUCTION

Various methods exist for the solution of thermal problems encountered in mechanical and civil engineering. Direct analytical methods can only be applied to a limited number of practical cases. In order to solve complicated problems in modern technical applications, it is almost necessary to adopt numerical procedures, i.e. finite differences or finite elements. In thermo-mechanical problems preference is generally given to finite elements, in order to take advantage of the same numerical scheme for the thermal and the mechanical problem.

A large number of numerical procedures have been described to solve various thermal problems.[1–6] However, for some particular cases, they do not always give a suitable or appropriate solution. Two particular questions are discussed hereafter.

In civil engineering, composite sections made of steel and concrete are often used. Beside the technical problems appearing when examining the mechanical behaviour of this type of structure, a particular question arises for the numerical solution of thermal problems. The composite section is made of a material with a high conductivity (steel) and a material with a low conductivity (concrete). Furthermore the steel profiles are made of elements with a small thickness. When an explicit numerical scheme is used in such a case, it is well known that severe conditions on the time step are encountered. As the massivity of the section is rather high, a large number of discrete elements has to be chosen together with a very large number of time steps. This may lead to prohibitive computation time, which explains why implicit numerical schemes are to be preferred.

Another problem encountered frequently in civil and mechanical engineering is the presence of internal voids. The deformation of concrete towers due to solar radiation, as well as the

CCC 0748–8025/94/060437–15

Received 2 August 1993
Revised 12 October 1993

fire resistance of steel elements protected with a box-casing insulation, or of hollow-core slabs, are problems of this type. This question is usually solved by using the concept of view factors,[7] but differences may appear in the way of discretizing the boundary of the cavity and of evaluating the influence of convection and radiation.

The application of this work to fire risk assessment problems must be pointed out. It gives a powerful tool to determine the temperature distribution under fire conditions in elements and structures with a complicated shape, but currently used in practice.

The aim of this paper is to present this new tool. A few numerical examples are described in order to show the capacity of the program and the influence of some parameters.

2. BASIC EQUATIONS AND BOUNDARY CONDITIONS

The balance equation governing the heat conduction in a solid can be written as follows:[8]

$$\nabla^{\mathrm{T}}(\mathbf{k}\,\nabla T) + Q_{\mathrm{v}} = \rho c \frac{\partial T}{\partial t} \tag{1}$$

where

$\nabla^{\mathrm{T}}(\mathbf{k}\,\nabla T)$ = balance of conduction flow

Q_{v} = internal heat generation

$\rho c(\partial T/\partial t)$ = heat accumulation

with $\nabla^{\mathrm{T}} = (\partial/\partial x, \partial/\partial y, \partial/\partial z)$

$\mathbf{k}$ = thermal conductivity tensor

T = temperature

ρ = volumetric mass

c = specific heat

t = time

In the present version of the code only 2D problems can be considered. In the case of a homogeneous and isotropic material, which is the situation most often encountered, equation (1) can be rewritten as

$$k(T)\cdot\Delta T + Q_{\mathrm{v}} = \rho c(T)\frac{\partial T}{\partial t}, \qquad \text{where} \qquad \Delta = \frac{\partial^2}{\partial x^2} + \frac{\partial^2}{\partial y^2} \tag{2}$$

However, the thermal properties k and ρc depend on the temperature, which is mandatory when high temperatures are reached as in fire problems, as confirmed by experimental results.

An important problem when concrete is involved and high temperatures reached is the evaporation of moisture inside the element. Usually this evaporation is taken into account, but mass transfer associated with this phenomenon is neglected. The same assumption has been made here. Several ways can be envisaged to treat this problem.

The first possibility is to keep the term Q_{v} in equation (1) and to calculate the quantity of heat absorbed during the evaporation process.[4,5,9] The second possibility consists in modifying the term ρc by increasing it substantially in the vicinity of 100° C, for example between 100 and 200° C.[10,11] Furthermore, in order to avoid steep changes in the law giving ρc with respect to temperature, it may be convenient to use the enthalpy formulation as in References 6 and 7. In this way the average variation of enthalpy $\Delta\bar{H}$ from temperature T_1 to temperature T_2

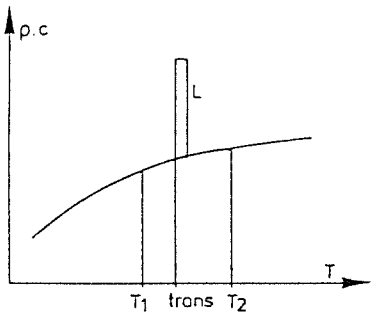

Figure 1. Evaporation of free water in concrete

can be written as follows (Figure 1):

$$\Delta\bar{H} = \frac{1}{T_2 - T_1}\left(\int_{T_1}^{T_2} \rho_c c_c(T)\, dT + \sum_i L_i\right) \tag{3}$$

where subscript c refers to concrete and L_i stands for latent volumetric heat due to phase changes at various temperature levels.

The initial condition determines the temperature distribution in the section at the reference time. The condition $T(x, y) = 20^\circ$ C for $t = 0$ is very often considered.

Boundary conditions refer to imposed temperature or imposed heat flow on the boundaries. Heat flow conditions will be examined hereafter.

The normal heat flow at the boundary can be written as follows:

$$\begin{aligned} q &= q_c + q_r = \text{convection} + \text{radiation} \\ &= \beta(T_s - T_f)^\gamma + \varepsilon\sigma(T_s^4 - T_f^4) \end{aligned} \tag{4}$$

where: β = coefficient of convection exchange
γ = power characterizing the convection exchange
ε = resultant emissivity
σ = Stefan–Boltzmann constant
T_s = absolute temperature of the surface
T_f = absolute temperature of the environment

A special type of boundary condition has also been defined for the internal boundary of a cavity in transient thermal equilibrium.

The specific heat of air is negligible with respect to that of solid materials. The temperature of the air is supposed to be uniform inside the cavity and it is assumed that there is no air movement towards or outwards of the cavity. The fictitious temperature of the air, T_f, can then be univocally determined by the global equilibrium of the convective flows on the boundary of the cavity, since the air in the cavity is assumed perfectly transparent to radiation

$$Q_c = \int_{\partial v} q_c\, ds = 0$$

or

$$\int_{\partial v} \beta(T_s - T_f)^\gamma\, ds = 0 \tag{5}$$

For an incident radiation striking the surface of a solid, it can be written, from a global equilibrium point of view, that:

$$\rho + \tau + \alpha = 1 \tag{6}$$

where ρ is the reflected part of the radiation, τ is the transmitted part and α is the absorbed part.

The internal surface of the cavity is considered as belonging to a perfectly diffusive gray and opaque body ($\tau = 0$). The emission and absorption depend neither on the incident angle nor on the wavelength (no specular or spectral effect). Kirchhoff's theory ensures for such a case that

$$\varepsilon = \alpha \tag{7}$$

Therefore, from relation (6),

$$\rho = 1 - \alpha = 1 - \varepsilon \tag{8}$$

3. FORMULATION BY FINITE-ELEMENT METHOD

In order to solve the problems of heat transfer taking into account the two particular matters hereabove mentioned (composite sections and internal voids), several contributions have been proposed. References 4 and 5 explain how a simple procedure based on finite differences is integrated in code CEFICOSS. Although several improvements have been made in Reference 5, it has some drawbacks—the large number of time steps to be used and the difficulty of modelling oblique and curved boundaries. FIRES T described in Reference 3 is mainly devoted to concrete structures. An important contribution has been presented by U. Wickström in TASEF 2[6,7] with a study of the effect of internal voids. However, the finite-element procedure is based on an explicit scheme of integration, and therefore is not appropriate for composite steel–concrete structures.

3.1. Temperature distribution in the solid

The new code described here and called THERMIN uses an isoparametric plane triangle with six nodes in order to model curved boundaries.

The matrix balance equation is obtained from the method of weighted residuals. Equation (1) is multiplied by a ponderation function w_i and integrated on the solid in order to verify on the average the thermal equilibrium on the volume,

$$\int_v w_i \cdot \left[-\nabla^{\mathrm{T}} \mathbf{k} \nabla T - Q_v + \rho c \frac{\partial T}{\partial t} \right] \mathrm{d}V = 0 \qquad (i = 1, 2 \ldots) \tag{9}$$

Galerkin's method introduces a set of ponderation functions w_i identical to the interpolation functions ϕ_i used to describe the temperature field:

$$\langle \tilde{w} \rangle = \langle \tilde{\phi} \rangle \qquad \text{and} \qquad T = \langle \tilde{\phi} \rangle \cdot \{ \tilde{\mathbf{T}} \} \tag{10}$$

in which $\langle\ \rangle$ denotes a line vector and $\{\ \}$ a column vector.

By using Green's theorem and various transformations, the following non-linear matrix equation can be obtained:[2]

$$[\tilde{\mathbf{K}}(T)]\{\tilde{\mathbf{T}}\} + [\tilde{\mathbf{C}}(T)]\{\dot{\tilde{\mathbf{T}}}\} = \{\tilde{\mathbf{g}}(T)\} \tag{11}$$

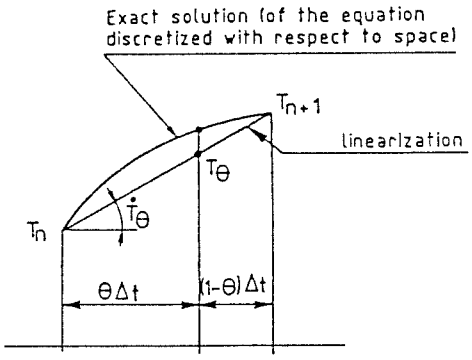

Figure 2. Linearization of solution

in which a superimposed dot stands for the time derivative and

$[\tilde{\mathbf{K}}]$ = conductivity matrix

$[\tilde{\mathbf{C}}]$ = capacity matrix

$\{\tilde{\mathbf{g}}\}$ = vector of heat flows at the nodes

$\{\tilde{\mathbf{T}}\}$ = vector of nodal temperatures

As already explained, an implicit integration scheme has been adopted in order to improve the total computation time taking into account the presence of concrete and steel.

Among the various formulations, the one expressing the thermal equilibrium at a particular time of the time interval $[t_n, t_{n+1}]$ has been chosen.[2]

The temperature is linearized in the time step $[t_n, t_{n+1}]$ by using the parameter α (cf. Figure 2):

$$\{\tilde{\mathbf{T}}_\alpha\} = (1-\alpha)\{\tilde{\mathbf{T}}_n\} + \alpha\{\tilde{\mathbf{T}}_{n+1}\} \qquad \text{with} \qquad \alpha \in [0,1] \tag{12}$$

and also its time derivative

$$\{\dot{\tilde{\mathbf{T}}}_\alpha\} = \left\{\frac{\partial \tilde{\mathbf{T}}_\alpha}{\partial t}\right\} = \left\{\frac{\tilde{\mathbf{T}}_{n+1} - \tilde{\mathbf{T}}_n}{\Delta t}\right\} = \left\{\frac{\tilde{\mathbf{T}}_\alpha - \tilde{\mathbf{T}}_n}{\alpha \Delta t}\right\} \tag{13}$$

where a subscript refers to a particular time, ($\{\tilde{\mathbf{T}}_n\} = \{\tilde{\mathbf{T}}(t_n)\}$).

The thermal equilibrium is realized at time

$$t_\alpha = (1-\alpha)t_n + \alpha t_{n+1} \tag{14}$$

Equation (9) can thus be written as follows:

$$[\tilde{\mathbf{K}}_\alpha]\{\tilde{\mathbf{T}}_\alpha\} + [\tilde{\mathbf{C}}_\alpha]\left\{\frac{\tilde{\mathbf{T}}_\alpha - \tilde{\mathbf{T}}_n}{\alpha \Delta t}\right\} = \{\tilde{\mathbf{g}}\} \tag{15}$$

The equilibrium can only be obtained by an iterative procedure such as Newton–Raphson.

3.2. Heat flow at the boundaries

The thermal load entering the solid at a particular node i of a boundary ∂V can be expressed as follows:

$$g_i^{\partial V} = \int_{\partial_V} \psi_i q(s)\, ds \tag{16}$$

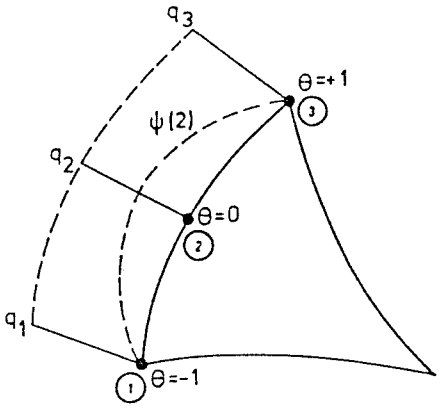

Figure 3. Heat flow at boundaries

with ψ_i being second-order shape functions depending on the reduced arc length θ $[-1, +1]$, such as

$$\psi = \begin{bmatrix} \psi_1 \\ \psi_2 \\ \psi_3 \end{bmatrix} = \frac{1}{4} \begin{bmatrix} -2\theta & (1-\theta) \\ 4(1+\theta) & (1-\theta) \\ 2\theta & (1+\theta) \end{bmatrix} \tag{17}$$

By making use of parameter θ instead of the curvilinear co-ordinate s, equation (16) can be rewritten in the following way (cf. Figure 3):

$$g_i^{\partial V} = \int_{-1}^{+1} \psi_i(\theta) q(\theta) \frac{\mathrm{d}s}{\mathrm{d}\theta} \, \mathrm{d}\theta \tag{18}$$

where $q(\theta)$ and $\mathrm{d}s/\mathrm{d}\theta$ can be related to the shape functions ψ_j and to the nodal heat flows q_j as follows:

$$q(\theta) = \sum_{j=1}^{3} \psi_j(\theta) q_j$$

$$q_j = \varepsilon\sigma(T_f^4 - T_j^4) + \beta(T_f - T_j)^{\gamma} \tag{19}$$

$$\frac{\mathrm{d}s}{\mathrm{d}\theta} = \left[\left(\frac{\mathrm{d}x}{\mathrm{d}\theta} \right)^2 + \left(\frac{\mathrm{d}y}{\mathrm{d}\theta} \right)^2 \right]^{1/2} = \left[\left(\sum_{j=1}^{3} \frac{\mathrm{d}\psi_j}{\mathrm{d}\theta} x_j \right)^2 + \left(\sum_{j=1}^{3} \frac{\mathrm{d}\psi_j}{\mathrm{d}\theta} y_j \right)^2 \right]^{1/2}$$

x_j and y_j being the nodal co-ordinates in the plane.

The following relation is therefore obtained:

$$g_i^{\partial V} = \sum_{j=1}^{3} \left[\int_{-1}^{+1} \psi_i(\theta) \psi_j(\theta) \frac{\mathrm{d}s}{\mathrm{d}\theta} \, \mathrm{d}\theta \right] q_j \tag{20}$$

$g_i^{\partial V}$ can then be calculated by using Gauss integration points on the boundary.

4. MODELLING OF HEAT EXCHANGES IN CAVITIES

Internal cavities are considered as particular cases. From the discretization the cavity is surrounded by a finite number of segments each having three nodes.

4.1. Convective exchanges

For the convective exchanges it is assumed that the air of the cavity has a well defined temperature, which corresponds to having a fictitious central node with temperature T_f (Figure 4). The specific heat of the air is assumed negligible with respect to the one of solid materials, and the mass of air is neglected. It is assumed that there is no air movement towards or outwards of the cavity. At the beginning of each time step, temperature T_f is calculated in such a way as to ensure equilibrium of the convective heat flows, the nodal temperatures being those calculated from the preceding time step.

In order to somewhat simplify the procedure the nodal convective flows are considered constant during the time step.

The convective heat balance inside the cavity is given by equation (5):

$$\sum_{i=1}^{N_{nc}} \int_{\partial CA} q_c(s)\, ds = \int_{\partial CA} \beta [T_s(s) - T_f]^\gamma\, ds = 0 \tag{21}$$

where ∂CA is the boundary of the cavity, and N_{nc} is the number of nodes on the boundary of the cavity.

Making use of equations (19), the convective heat balance can be written according to equation (20) in the following way:

$$\sum_{i=1}^{N_{nc}} \sum_{j=1}^{3} \left[\int_{-1}^{+1} \psi_i(\theta)\psi_j(\theta) \frac{ds}{d\theta}\, d\theta \right] q_{cj} = 0 \tag{22}$$

The term

$$\left[\int_{-1}^{+1} \psi_i(\theta)\psi_j(\theta) \frac{ds}{d\theta}\, d\theta \right]$$

is calculated only once by Gauss integration, and getting T_f from equation (22) is made in an iterative manner.

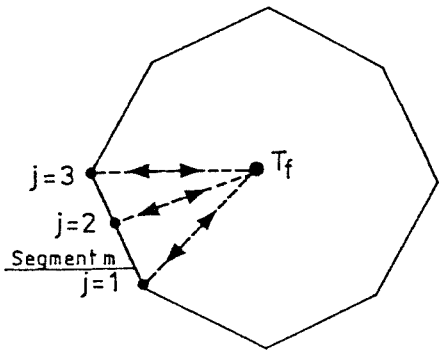

Figure 4. Boundaries of a cavity and fictitious central node

4.2. Radiative exchanges[2]

The first problem to be solved is the determination of the effective radiative heat flow q_{rm} derived from the thermal balance at segment m. This can be expressed by the following

relation:

$$q_{rm} = \varepsilon_m \sigma T_m^4 - \alpha_m H_m$$
$$= \varepsilon_m \sigma T_m^4 - \varepsilon_m H_m \tag{23}$$

where H_m is the radiative heat flow striking segment m.

The radiative heat flow H_m striking segment m is a function of the flows R_n leaving all the segments n surrounding segment m. These flows R_n depend on the emissivity and on the reflectivity of surface n. Therefore,

$$R_n = \varepsilon_n \sigma T_n^4 + \rho_n H_n$$
$$= \varepsilon_n \sigma T_n^4 + (1 - \varepsilon_n) H_n \tag{24}$$

R_n is called the radiosity of segment n.

Between R and H the following relation exists:

$$H_m = \sum_{n=1}^{N_s} F_{mn} R_n \tag{25}$$

where N_s is the number of segments of the cavity, and F_{mn} is the view factor of face m towards face n.

The view factors are calculated automatically in 2D cases by Hottel's rule (cf. Figure 5), and are given by

$$F_{mn} = \frac{L_{AD} + L_{BC} - L_{AC} - L_{BD}}{2L_{AB}} \tag{26}$$

By eliminating H_m and R_n between equations (23), (24) and (25), one obtains

$$\sum_{n=1}^{N_s} \left[\frac{\delta_{mn}}{\varepsilon_n} - F_{mn} \frac{1 - \varepsilon_n}{\varepsilon_n} \right] q_{rn} = \sum_{n=1}^{N_s} [\delta_{mn} - F_{mn}] \sigma T_n^4 \tag{27}$$

which can be written in matrix form as:

$$[\tilde{\mathbf{X}}]\{\tilde{\mathbf{q}}_r\} = [\tilde{\mathbf{Y}}]\sigma\{\tilde{\mathbf{T}}^4\} \tag{28}$$

where matrices $[\tilde{\mathbf{X}}]$ and $[\tilde{\mathbf{Y}}]$ are calculated only once.

By knowing the mean temperature of each segment it is possible to find directly the flow exchanged by this segment from

$$\{\tilde{\mathbf{q}}_r\} = [\tilde{\mathbf{X}}]^{-1}[\tilde{\mathbf{Y}}]\sigma\{\tilde{\mathbf{T}}^4\} \tag{29}$$

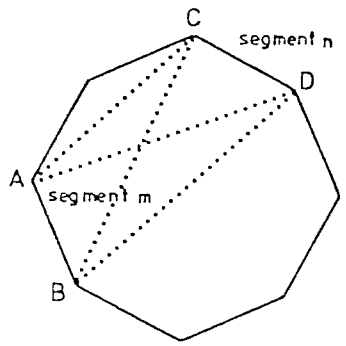

Figure 5. Calculation of view factors by Hottel's rule

The nodal radiative thermal loads are then calculated from these uniform flows q_{rm} by making use of equation (18) in the following way:

$$g_{ri}^{\partial CA} = \int_{\partial CA} \psi_i q_{rm} \, ds$$

$$= q_{rm} \int_{-1}^{+1} \psi_i(\theta) \frac{ds}{d\theta} \, d\theta \tag{30}$$

which can be again evaluated by using Gauss integration points, considering q_{rm} spatially constant on edge m.

For the application of the preceding procedure a few restrictions exist:

- the cavity must be convex and without internal obstacle (all interior angles between surfaces $\leqslant 180^\circ$ for a total mutual vision)
- the cavity must be closed (the temperature of all the surfaces must be defined).

5. PRACTICAL EXAMPLES

In order to show the capacity of the program, two practical examples are presented.

5.1. Example 1: Composite steel–concrete column without internal cavity

The first one refers to a composite steel–concrete column specially developed for buildings with severe fire resistance requirements[9] (cf. Figure 6). The values adopted for the parameters defining the heat exchange are indicated in Figure 6. The thermal characteristics adopted for steel and concrete are those proposed in Eurocode 2 and 4 – Part 10.[10,11]

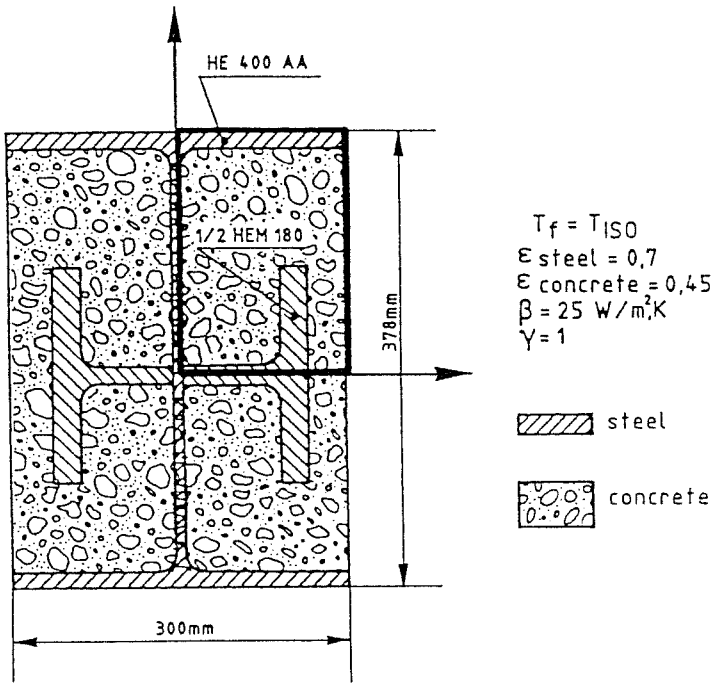

Figure 6. Composite AF rectangular column (HE profiles)

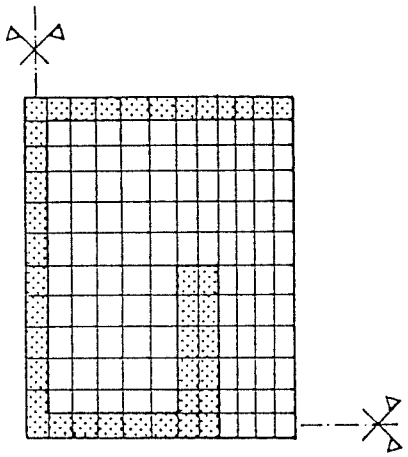

Figure 7. Discretization of the quarter of the cross-section by CEFICOSS (cf. Figure 6)

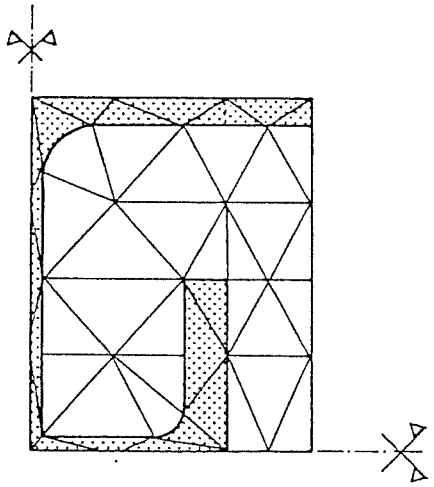

Figure 8. Discretization of a quarter of the cross-section by THERMIN (cf. Figure 6)

Because of symmetry conditions it is possible to model only a quarter of the cross-section. The discretizations adopted with CEFICOSS and THERMIN are presented in Figures 7 and 8, respectively. It can be seen that the number of elements is much smaller with THERMIN. The curved boundaries of the profile can be taken into account, which is not possible with CEFICOSS.

Figure 9 shows a comparison between experimental results obtained by thermocouples situated near the flanges of the profile, and numerical results obtained by CEFICOSS and by THERMIN. Theoretically the results given by the thermocouples should be identical. Both numerical results are quite satisfactory; the agreement is somewhat better with THERMIN considering the average given by experimental results.

It is interesting to have a look at the temperature distribution in the composite profile after 2 h of ISO standard fire (Figure 10). It can be seen that near the boundaries the temperature

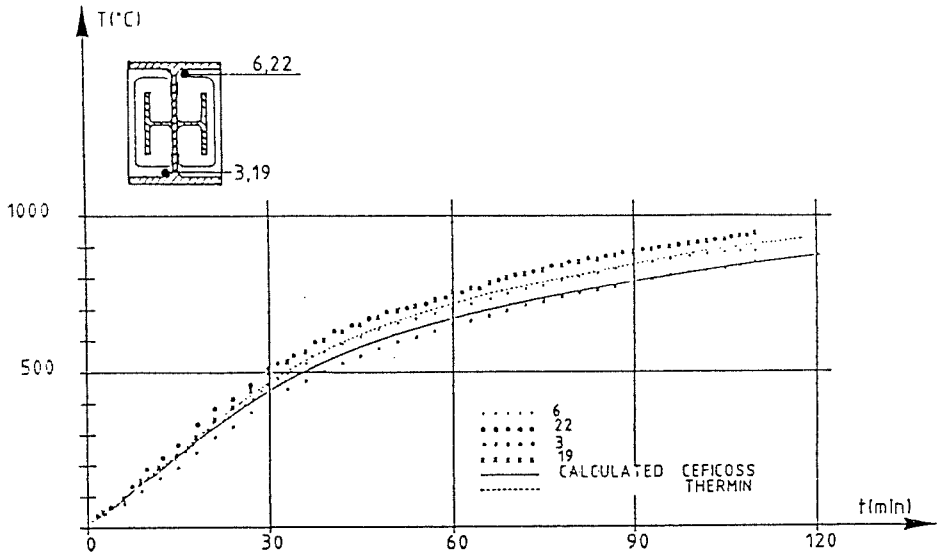

Figure 9. Comparison between calculated and measured temperatures

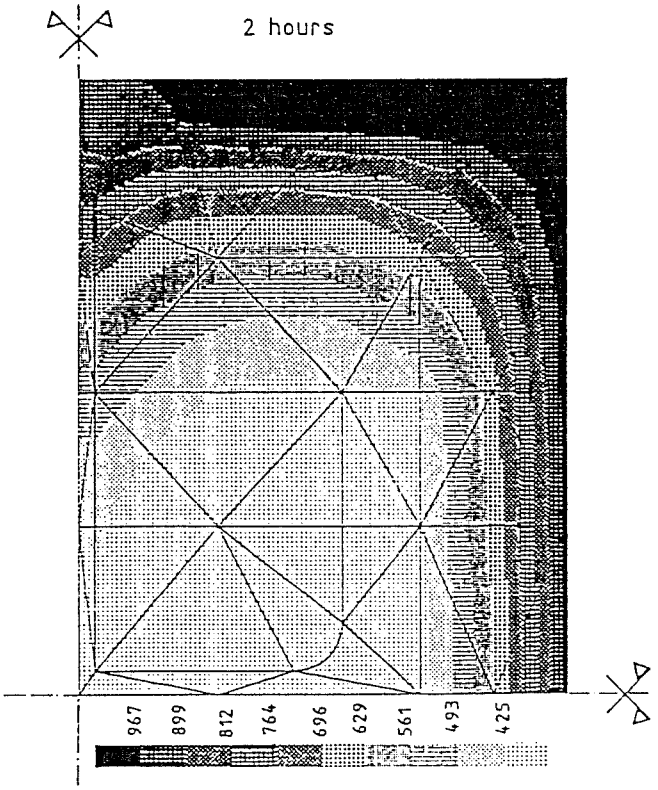

Figure 10. Temperature distribution in composite profile

is very high ($\geqslant 1000^\circ$ C), while the centre remains rather cold. The influence of the web of the HEA profile on the temperature distribution can also be noted; owing to its high conductivity the penetration of the heat inside the profile is more important in this area.

5.2. Example 2: Prestressed concrete slab with internal voids

The second practical example is devoted to a prestressed concrete slab with internal voids (Figure 11). This type of slab is probably the most often used for floors in building construction. However, the influence of the voids on the fire resistance of the slab is still under

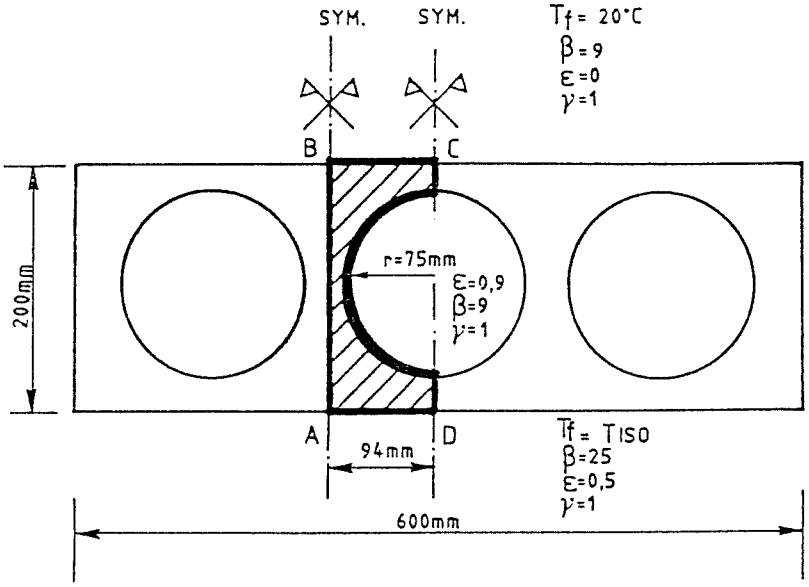

Figure 11. Prestressed concrete slab with internal voids

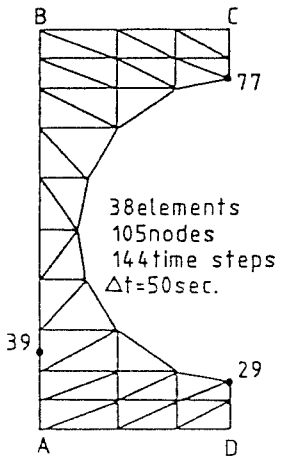

Figure 12. Discretization of part ABCD (cf. Figure 11)

discussion[10] because very few models have been developed for the evaluation of the temperature distribution inside the element.

The dimensions of the slab are indicated in Figure 11 as well as the values adopted for the parameters defining the heat exchange. Numerical results can be obtained by considering zone ABCD only. The discretization adopted for this part is indicated in Figure 12.

Figure 13 shows the temperature increase at various points of the cross-section obtained by THERMIN. Nodes 29 and 77 correspond to the bottom and top of the cavity, while node 39

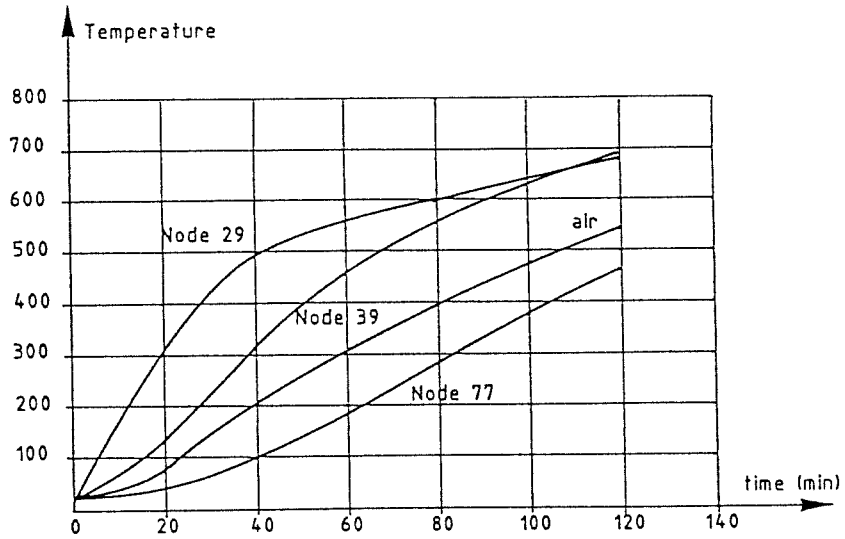

Figure 13. Calculated temperature increase at various points of cross-section

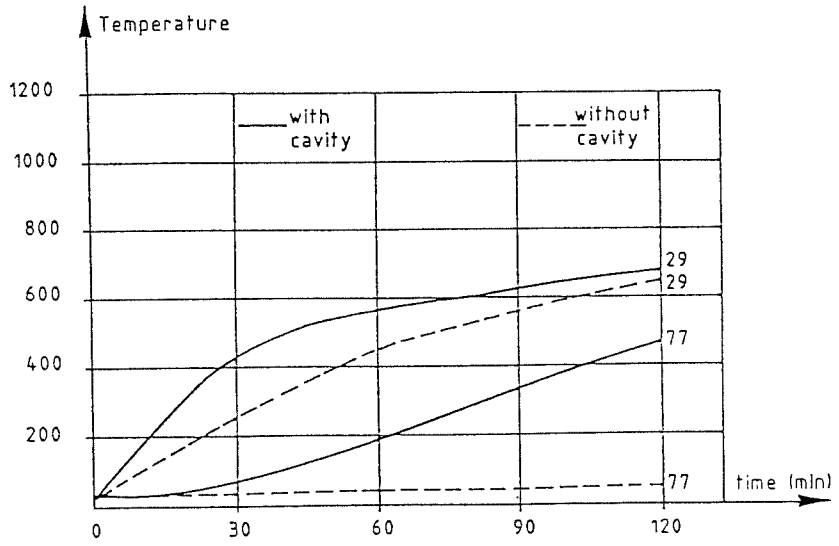

Figure 14. Calculated temperature increase for various cases

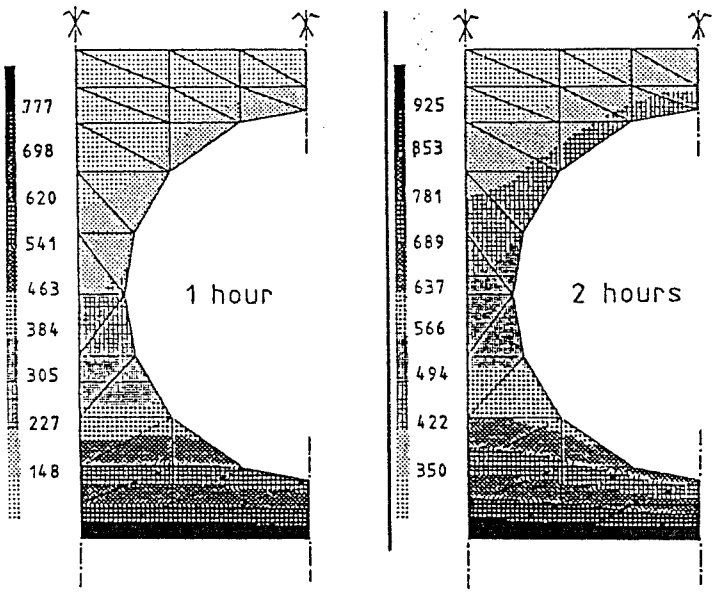

Figure 15. Temperature distribution in slab

corresponds approximately to the position of the prestressing tendons; the temperature at this point is thus determinant for the fire endurance of the slab. The conventional temperature of the air inside the cavity is also represented. It can be seen that the temperature difference between the bottom and the top of the cavity is very high.

In Figure 14 a comparison is made between the same theoretical results and those obtained for a slab without cavity. It can be seen that at the bottom of the slab (node 29), the difference is important after 30 and 60 min, but after 90 and 120 min the difference is less significant; at the top of the slab (node 77), the difference is very important.

The temperature distribution in the slab after 1 and 2 h of ISO standard fire is represented in Figure 15.

6. CONCLUSIONS

In this article a computation code for the thermal analysis of structures has been presented. Various thermal actions and, more particularly, fire conditions can be envisaged.

It is well adapted for the evaluation of the temperature distribution in composite structures and in elements with internal cavities.

The use of composite sections made of materials with low and high thermal conductivities has led to adopting an implicit scheme for the numerical solution. More specifically the case of composite steel–concrete sections has been considered.

A simple and efficient procedure has been developed in order to treat the presence of internal cavities.

In order to show the capacity of the program, two practical examples have been described. There is good agreement between theoretical results obtained from this code and experimental results, and also theoretical results obtained from another computer code.

REFERENCES

1. E. L. Wilson and A. E. Nickell, 'Application of the finite element method to heat conduction analysis', *Nucl. Eng. & Des.*, **4**, 276–286 (1966).
2. M. Hogge, 'Modélisation des transferts de chaleur et de matière', Notes de cours, Université de Liège, 1985.
3. J. Becker, H. Bizri and B. Bresler, 'FIRES T. A computer program for the fire response of structures', Report N° UCB FRG 74-1, University of California, Berkeley, 1974.
4. J.-C. Dotreppe, 'Méthodes numériques pour la simulation du comportement au feu des structures en acier et en béton armé', Thèse d'agrégation de l'enseignement supérieur, Université de Liège, 1980.
5. J.-M. Franssen, 'Etude du comportement au feu des structures mixtes acier-béton', Thèse de doctorat, Université de Liège, 1986.
6. U. Wickström, 'TASEF 2 – A computer program for temperature analysis of structures exposed to fire', Report N°79-2, Department of Structural Mechanics, Lund, Sweden, 1979.
7. U. Wickström, 'A numerical procedure for calculating temperature in hollow structures exposed to fire', Report N°79-3, Department of Structural Mechanics, Lund, Sweden, 1979.
8. H. S. Carslaw and J. C. Jaeger, *Conduction of Heat in Solids*, 2 Edn, Clarendon Press, Oxford, 1959.
9. J. B. Schleich, J.-M. Franssen and J.-C. Dotreppe, 'Analyse de la résistance au feu des structures en acier et mixtes béton-acier, assistée par ordinateur (REFAO-CAFIR)', Rapport final, Convention C.C.E. N°7210-SA/502, 1986.
10. C.E.C., 'Eurocode n°2 – Design of concrete stuctures – Part 10: Structural fire design', Draft April 1990, C.E.C., Bruxelles, 1990.
11. C.E.C., 'Eurocode n°4 – Design of composite structures – Part 10: Structural fire design', Draft April 1990, C.E.C., Bruxelles, 1990.